JOURNAL OF AIRCRAFT
Vol. 39, No. 1, January–February 2002

# Structural Optimization of a Hat-Stiffened Panel Using Response Surfaces

Roberto Vitali,* Oung Park,* Raphael T. Haftka,† and Bhavani V. Sankar‡
*University of Florida, Gainesville, Florida 32611-6250*
and
Cheryl A. Rose§
*NASA Langley Research Center, Hampton, Virginia 23681-2199*

**A design study for structural optimization of a hat-stiffened laminated composite panel concept for an upper cover panel of a typical passenger bay of a blended wing–body transport airplane configuration is described. The feasibility of a hat-stiffened composite panel concept for an upper cover panel is investigated and is compared on the basis of weight to a thick sandwich panel concept that has been selected by designers as the baseline concept for the upper cover panel. The upper cover panel is designed for two load cases: internal pressure only and combined internal pressure and spanwise compression due to wing bending. The structural optimization problem is formulated using the panel weight as the objective function, with constraints on stress and buckling. The spacing of the hat stiffeners, the thickness of the skin, and the thickness of the components of the hat stiffener are used as design variables. The initial geometry of the hat-stiffened panel design is determined using the PANDA2 program by restricting the design to have uniform cross section in the spanwise direction. Because of the pressure loading, a more efficient design has variable cross section. Such designs are obtained by combining the STAGS finite element program with the optimization program in the Microsoft EXCEL spreadsheet program using response surfaces. Buckling and stress response surfaces are constructed from multiple STAGS analyses and are used as constraints in the optimization. The optimization conducted with the response surfaces results in considerable weight savings compared to the uniform cross section design, albeit a more complex design. Initial optimization cycles identify a design space where simple approximate analyses, such as Euler–Bernoulli beam theory and Kirchhoff plate theory applied to laminated composites, can be used to predict the behavior of the structure.**

## Introduction

MAJOR air carriers have expressed the need for larger airplanes to meet the growing demands for air travel, especially in the Pacific Rim and on transatlantic routes between major airports in the United States and Europe. A blended wing–body (BWB) 800-passenger aircraft is one of several configurations currently being considered for satisfying this need. As the name implies, a principal feature of a BWB transport is a wide double-deck centerbody that is blended into the wing. Because of the shape of the airplane, the pressurized centerbody region, which includes both the passenger area and the cargo area, is noncircular (see Fig. 1). The noncircular centerbody region has several challenging issues from the standpoint of structural design because the upper and lower cover panels carry the overall aircraft body moments ($M_x$ in Fig. 1) internal pressure, and wing bending moments ($M_y$ in Fig. 1). To reduce instability problems in the upper cover panel, which is subjected to compressive running loads due to wing bending, and to reduce bending stresses due to the internal pressure loading, the inboard centerbody section is divided into several passenger and cargo bays, which are separated by chordwise ribs. A typical passenger bay is 150 in. wide, as shown in Fig. 1.

Received 28 May 1999; revision received 29 March 2001; accepted for publication 20 April 2001. 

*Graduate Research Assistant, Department of Aerospace Engineering, Mechanics, and Engineering Science, 231 Aerospace Building. Student Member AIAA.

†Distinguished Professor, Department of Aerospace Engineering, Mechanics and Engineering Science. 231 Aerospace Building. Fellow AIAA.

‡Professor, Department of Aerospace Engineering, Mechanics and Engineering Science, 231 Aerospace Building. Associate Fellow AIAA.

§Senior Engineer, Mechanics and Durability Branch, Mail Stop 190. Member AIAA.

A variety of structural configurations for the pressurized upper cover panel structure were considered as part of a BWB design study. The configurations that were considered in the study include conventional skin-stringer constructions, deep sandwich structure, and separate structures for carrying the internal pressure and wing bending loads. A deep sandwich configuration was chosen as the baseline structure on the basis of low weight combined with ease of fabrication and assembly. However, some unresolved issues of sandwich structures might prevent their use as the primary structure for a BWB airplane. The present paper describes a structural optimization study of one of the alternative structural concepts being considered for the upper cover panel of a typical passenger bay of a BWB transport airplane. Specifically, results are presented for a composite hat-stiffened skin panel configuration. The skin and all of the components of the hat stiffener are built up from graphite–epoxy, warp-knit preforms. Each preform is a stack of material equivalent to seven layers of unidirectional prepreg with 0-, 45-, and 90-deg fibers and has a cured thickness of 0.055 ins. The loading cases used in this preliminary study did not include $M_x$ shown in Fig. 1. The wing bending moment $M_y$ was transformed into equivalent $N_x$ compressive and tensile running loads in the upper and lower cover panels, respectively. A comparison was made on the weight of the upper cover panel obtained for the hat-stiffened panel concept and for the thick sandwich concept for the load cases considered in this study. A hat-stiffened panel design was considered to be a valid alternative to the sandwich panel design if the weight of the hat-stiffened panel was equal to or less than 3.0 lb/ft$^2$.

The structural optimization problem is formulated using the panel weight as the objective function, with stress and buckling constraints. The spacing of the hat stiffeners, the thickness of the skin, and the thickness of the components of the hat stiffener are used as design variables. The thickness variables are integer multiples of the thickness of the basic composite material stack just described. Therefore, the optimization problem is discrete. Furthermore, the structural analyses required to evaluate the constraints are performed

by an analysis code that does not have optimization capabilities and that is difficult to interface with an optimization program. For such situations, response surface techniques, which create simple approximations of structural responses, have been shown to be useful.[1] Response surface techniques also permit simple analysis models to be integrated with more complex analysis models. In the present work, both simple and complex analysis models are integrated in response surfaces that are used in the structural optimization.

## Problem Description

The structural configuration considered in the optimization problem is a hat-stiffened skin, upper cover panel of a typical passenger bay, as shown in Fig. 2. The panel is 150 in. long in the spanwise $x$ direction, and 900 in. long in the chordwise $y$ direction. Two representative loading conditions are considered in the design. The first loading condition is combined internal pressure and spanwise $x$ compression. The second loading condition is internal pressure only. The two load cases considered do not have a load component in the chordwise direction. These two simple loading conditions were considered to be sufficient for obtaining a comparison of preliminary design concepts for the upper cover panel. The ends of the stiffened panel at $x = 0$ in. and at $x = 150$ in. are clamped. The clamped boundary condition is achieved by two simple support boundary conditions applied to the base and to the crown of the stiffener. The end of the panel at $x = 0$ in. is restrained from movement in the $x$ direction, and the opposite end of the panel at $x = 150$ in. is constrained to have a uniform $u$ displacement. The unloaded edges of the panel at $y = 0$ in. and at $y = 900$ in. are simply supported with an unconstrained $v$-displacement component.

The skin and the individual components of the hat stiffener are constructed from graphite–epoxy warp-knit preforms, which were developed under several NASA contracts.[2] Each preform is a stack of material equivalent to seven layers of unidirectional prepeg with 0-, 45-, and 90-deg fibers. The nominal stacking sequence of the preforms used in the skin and in all of the components of the hat stiffener is [45/−45/0/90/0/−45/45]. Each preform, or stack, has a cured thickness of 0.055 in. Nominal material properties for a cured stack and the stress allowables that are used in the designs are provided in Table 1.

## Structural Optimization

An initial optimum structural design for the upper cover panel was obtained using the PANDA2 program.[3] A refined optimum structural design was then obtained by an optimization using response surface techniques. The analyses required to construct the response surfaces were performed using both simple and complex analysis models. The complex structural analyses were performed using the STAGS[4] finite element program. The initial design was obtained for a combined load case of internal pressure, $p = 14.84$ psi, and spanwise compression, $N_x = -4319$ lb/in. The optimization for the initial load case is described in the sections "Design Using PANDA2 for Initial Load Condition" and "Design Using Response

**Table 1 Material properties for graphite–epoxy preforms**

| Property | Value |
|---|---|
| $E_{11}$, msi | 9.25 |
| $E_{22}$, msi | 4.67 |
| $G_{12}$, msi | 2.27 |
| $\nu_{12}$ | 0.397 |
| $\varepsilon_{all}$ | $5.40 \times 10^{-3}$ |
| $\sigma_{all}$, ksi | 50 |
| $\tau_{all}$, ksi | 18 |
| $\rho$, lb/in.$^3$ | 0.0057 |

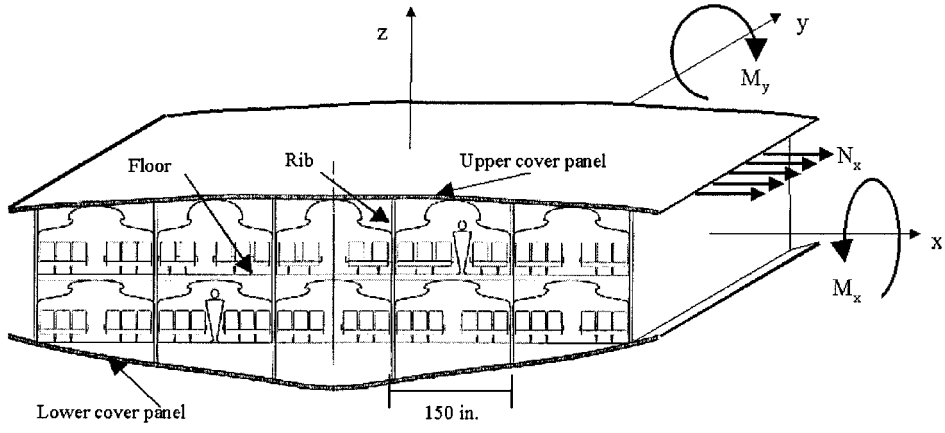


**Fig. 1 Center-body region of BWB transport airplane.**

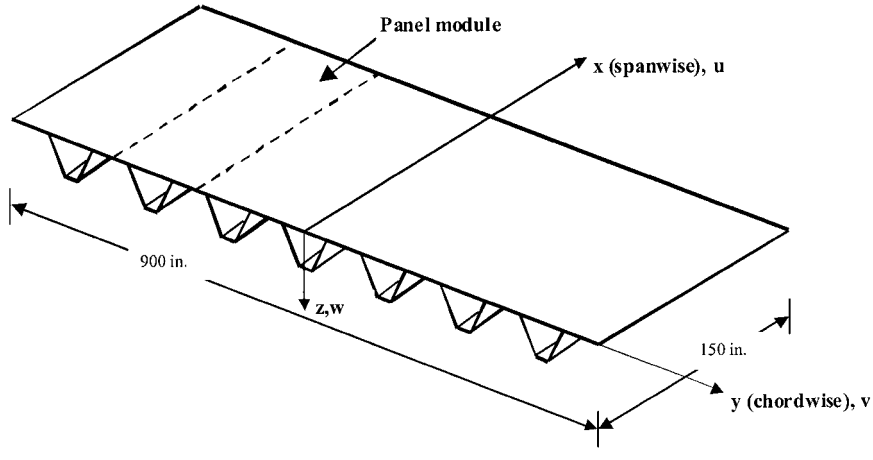


**Fig. 2 Hat-stiffened skin upper cover panel.**

Surface Techniques for Initial Load Condition." As the airplane design evolved, the design loads for the combined load case were updated to internal pressure $p = 15.59$ psi and spanwise compression $N_x = -2879$ lb/in., and an additional load case of internal pressure only, $p = 18.56$ psi, was added. The optimum structural design obtained for the initial combined load case was used as the starting point in the optimization problem for the updated load conditions. The design for the updated load conditions is described in the section "Design for Updated Load Conditions." A flow chart of the different hat-stiffened cover panel structures obtained during the optimization is shown in Fig. 3.

## Design Using PANDA2 for Initial Load Condition

The first step in the structural optimization was to use the PANDA2 program to obtain an initial design. PANDA2 was developed specifically to find minimum weight designs for stiffened, flat or curved panels, or complete cylindrical shells made of laminated composite materials. The stiffeners may run in one or two orthogonal directions, and all stiffeners in one direction are assumed to be identical and uniformly spaced. The panels can be loaded with combinations of in-plane loads, edge moments, normal pressure, and temperature. Constraints on the design include global and local buckling, stiffener crippling, maximum displacement due to internal pressure loading, maximum tensile or compressive stress along the fiber and normal to the fibers in each lamina, and maximum in-plane shear stress in each lamina. PANDA2 calculates local and general buckling load factors employing simple closed-form expressions and inexpensive finite difference analyses of discretized models of panel cross sections. Local buckling is predicted from the analysis of a single panel module, which is assumed to repeat several times over the panel width. A single panel module consists of one stiffener plus the panel skin, with width equal to the spacing between stiffeners. For a typical stiffener, PANDA2 finds the axial location in which each element of the panel module has the highest compressive stresses and performs a stability analysis based on these values. The results of the stability analysis are then used to size each element of the panel module.

In the present problem, the stiffeners run in the spanwise $x$ direction, and the panel consists of repetitive modules in the chordwise $y$ direction (Fig. 2). Furthermore, the properties of the panel are assumed to be uniform in the spanwise $x$ direction. A cross section of a panel module and the design variables used in the PANDA2 optimization are shown in Fig. 4. The objective function, the design variables, and the side constraints used in the PANDA2 optimization are listed in Table 2. The first constraint shown in Table 2 ensures that there are enough equally spaced stiffeners in the panel for a single module model to give a good approximation to the local skin buckling mode. The second and third constraints are recommended by the PANDA2 user's guide to guarantee numerical stability in

**Table 2 PANDA2 optimization problem (dimensions in inches)[a]**

| Side constraints | Constraint no. |
|---|---|
| $6 \le b \le 24$ | 1 |
| $b_2 - 0.75b \ge 0$ | 2 |
| $4.5 \le b_2 \le 18$ | 3 |
| $2 \le h \le 6.5$ | 4 |
| $b_2 - w_2 \ge 2.6$ | 5 |
| $2.9 \le w_2 \le 15.4$ | 6 |
| $2.25 \le w \le 11.75$ | 7 |
| $0.11 \le t \le 1.1$ | 8 |
| Buckling and stress constraints in PANDA2 | 9 |

[a] Objective function: min{weight}; design variables: $b, b_2, w, w_2, h, t_s, t_f, t_w, t_c$ see Fig. 4.

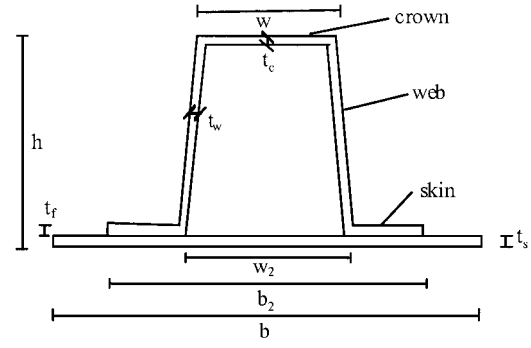


**Fig. 4 Cross section of single panel module and design variables used in PANDA2 optimization.**

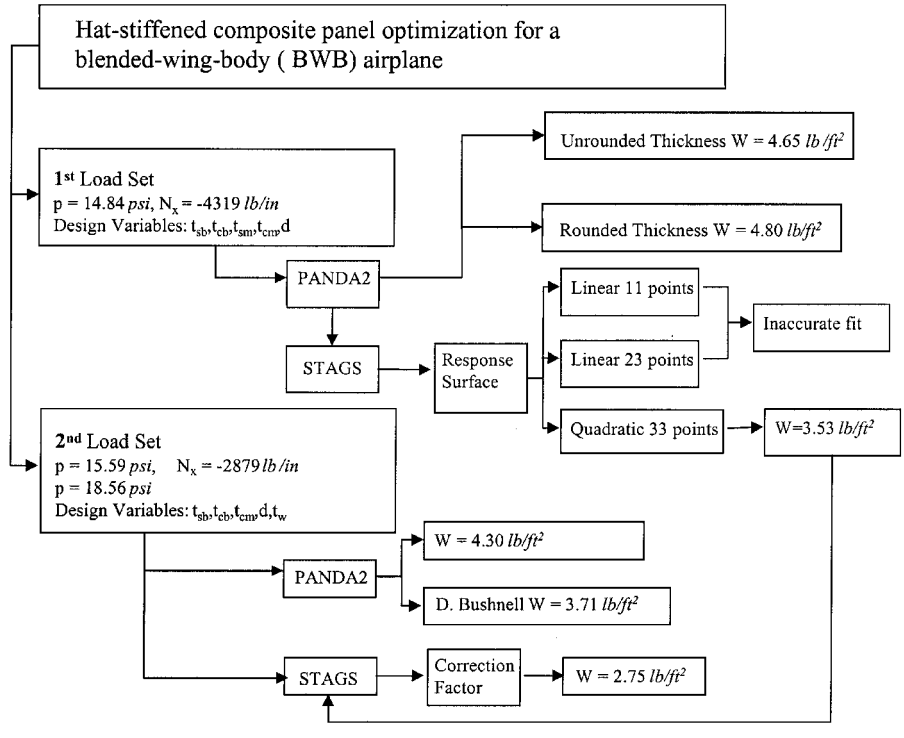


**Fig. 3 Flow chart of optimization history of hat-stiffened panel.**

**Table 3 PANDA2 original and rounded optimum design**

| Variable | Original | Rounded |
|---|---|---|
| Weight, lb/ft$^2$ | 4.65 | 4.86 |
| $b$, in. | 13.83 | 13.83 |
| $b_2$, in. | 8.4 | 8.4 |
| $h$, in. | 6.5 | 6.5 |
| $w$, in. | 4.3 | 4.3 |
| $w_2$, in. | 5.8 | 5.8 |
| $t_s$, in. | 0.22 | 0.22 |
| $t_f$, in. | 0.34 | 0.33 |
| $t_w$, in. | 0.20 | 0.22 |
| $t_c$, in. | 0.33 | 0.33 |

the solution procedure. The fourth constraint controls the height of the hat stiffener, where the upper value reflects a manufacturing limitation. The fifth and sixth constraints ensure that the flange is at least 1.3 in. wide, again for manufacturing reasons, and the seventh constraint ensures that the hat stiffeners have reasonable proportions. Finally, the eighth constraint sets the upper and lower thickness bounds for the panel skin and of all elements of the hat stiffener. Additional constraints on the design included global and local buckling, crippling, stiffener pop-off, maximum stresses along and normal to the fibers in each lamina, and maximum in-plane shear stresses within each element of the stiffener. In evaluating the constraints, a factor of safety equal to 1.3 was applied to the stresses and a factor of safety equal to 1.15 was applied to the buckling load factor. The buckling load safety factor reflects a design requirement that the structure will not buckle between design limit load and design ultimate load.

The optimum design for the hat-stiffened upper cover panel obtained by the PANDA2 program is provided in the second column in Table 3. As shown in Table 3, the optimum design obtained by the PANDA2 program weighed 4.65 lb/ft$^2$. The optimum design obtained by PANDA2 features continuous design variables. However, the thickness of the panel skin and the thickness of the individual components of the hat stiffener are discrete variables because the thicknesses are limited to integer multiples of the thickness of one warp-knit preform. Therefore, the optimum design obtained by PANDA2 must be rounded to the next feasible value of the discrete design variables. Rounding off the thicknesses to the nearest discrete thicknesses increased the weight of the cover panel to 4.86 lb/ft$^2$. The rounded-off design is shown in the third column of Table 3. For the rounded-off design shown, the active constraints at the mid-length of the panel were fiber compression in the crown, web buckling, and axial (spanwise direction) strain in the crown. At the ends of the panel, the active constraints included local buckling of the panel skin between the hat stiffeners, local buckling of the panel skin under the hats, and spanwise compression in the panel skin.

## Design Using Response-Surface Techniques for Initial Load Condition

For the loading and boundary conditions of the current problem, the design obtained with PANDA2 is conservative. The conservative design results from the imposed requirement that the panel properties are constant in the spanwise direction, whereas the loading for the present problem is variable in the spanwise direction.

A more efficient design for the stiffened panel was obtained by allowing the cross section of the panel to vary in the spanwise direction. Based on the results of the PANDA2 analysis, the panel was divided into three sections: two identical sections at the ends of the panel and a section in the interior of the panel, as shown in Fig. 5. The tendency of the skin to buckle near the ends of the panel, which was an active constraint in the PANDA2 analysis, was reduced by adding a layer of material equal to the thickness of the flange to the panel skin between the hat stiffeners and to the panel skin under the hat stiffeners. Furthermore, the thickness of the crown of the hat stiffeners in the end sections of the panel was allowed to be different than the thickness of the crown of the hat stiffeners in the interior region of the panel. The cross sections of a panel module in the

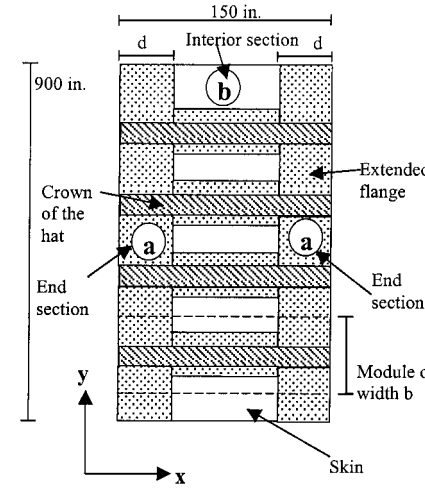


**Fig. 5 Division of hat-stiffened panel into three spanwise sections.**

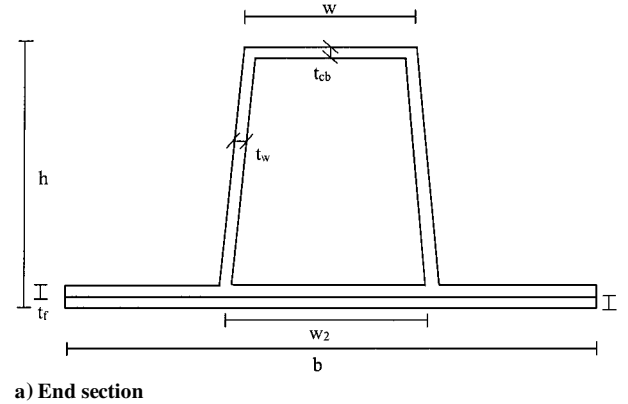


**a) End section**

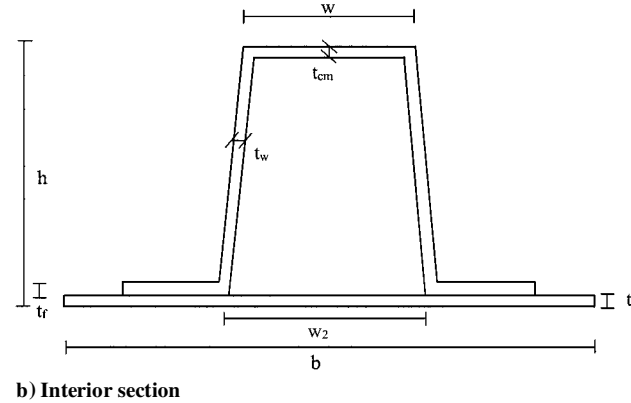


**b) Interior section**

**Fig. 6 Cross-sectional geometry of a variable-thickness panel.**

end sections of the panel and in the interior section of the panel are shown in Figs. 6a and 6b, respectively.

The STAGS[4] program was used to obtain accurate buckling loads and stress predictions for the variable cross-section panel shown in Figs. 5 and 6. STAGS is a finite element code for the nonlinear analysis of general shell structures of arbitrary shape and complexity. STAGS, however, does not have an optimization capability. Response-surface techniques, which create simple approximations of structural response, have been shown to be useful for design optimization when the design variables are discrete and when it is difficult to integrate the analysis and optimization codes. Response-surface methodology is used to obtain a relationship between a specified response variable (dependent variable) and the design (independent) variables. The response-surface model describes this relationship. In the current study, STAGS finite element analyses were used to construct response-surface models to approximate the panel buckling response and to approximate the midsurface compressive,

spanwise, skin stress in the thin skin section at the thickness discontinuity between the end and the interior regions of the panel. There was very little difference between the stresses on the outer surface of the skin and the inner surface of the skin at the discontinuity between the end and the interior regions of the panel; therefore, the midsurface stresses were compared with the maximum stress allowable. For the first loading condition considered in this study, the thickness discontinuity was the only region in the hat-stiffened panel where the stress constraint was violated. The response surfaces created were then used as constraint functions in an optimization procedure to minimize the panel weight. The optimization was performed using a spreadsheet in the Microsoft EXCEL[5] software program that allows discrete design variables. The optimization module in EXCEL, called SOLVER, is available in several other spreadsheet programs. The design variables used in the optimization are given in Table 4. The thickness of the flange ($t_f = 0.11$ in.) and the thickness of the web ($t_w = 0.22$ in.) were kept constant during the optimization process. The variables $h$, $w$, $w_2$, $b$, and $b_2$ were also held constant during the optimization process and were equal to the values given in Table 3.

Both the buckling response surface and the stress response surface were approximated using polynomials. A least-squares estimate of the unknown coefficients in the polynomials was obtained by evaluating the structural response (panel buckling load or stress at the thickness discontinuity) at a number of design points that exceeded the number of coefficients in the approximating polynomials. The structural response at the individual design points was determined using the STAGS finite element code. The method of analysis used to perform the stress and buckling analyses was linear. In particular, the buckling analysis was conducted by performing a linear bifurcation buckling analysis from a linear prestress state. The internal pressure $p$ and the in-plane load $N_x$ were included on the same load set so that the buckling load factor was applied to both loads. In all of the STAGS analyses, an additional factor of safety equal to 1.25 was applied to the end load so that a spanwise compression load, $N_x = 5398$ lb/in., was used.

To keep the cost of constructing a response surface as low as possible while ensuring the accuracy of the response-surface model, care must be taken in selecting the design points. Several methods are available for selecting the design points so that the error in the approximation is minimized. In the present study, the $D$-optimality criterion,[6] as implemented in the JMP program,[7] was employed to select the design points. The implementation in the JMP program finds a $D$-optimal set of points from a given set of candidate design points in the design domain. The 9604 candidate design points that were used for constructing the response surfaces are defined in Table 5. Also given in Table 5 is a nominal design, selected by engineering judgment. The nominal design weighs 3.741 lb/ft$^2$, has a buckling load factor applied to both the internal pressure and compressive running loads of 1.898, and has spanwise, compressive mid-surface stress in the thin skin section at the thickness discontinuity equal to 20,288 psi.

**Table 4 Design variables used in response surface optimization**

| Variable | Variable meaning |
|---|---|
| $d$ | Distance from panel ends to thickness discontinuity |
| $t_{sb}$ | Skin thickness in end sections |
| $t_{sm}$ | Skin thickness in interior section |
| $t_{cb}$ | Crown thickness in end sections |
| $t_{cm}$ | Crown thickness in interior section |

**Table 5 Candidate points for response surface construction**

| Design variable | Minimum, in. | Step, in. | Maximum, in. | Nominal design, in. |
|---|---|---|---|---|
| $d$ | 12 | 12 | 48 | 36 |
| $t_{sb}$ | 0.110 | 0.055 | 0.440 | 0.165 |
| $t_{sm}$ | 0.110 | 0.055 | 0.440 | 0.110 |
| $t_{cb}$ | 0.110 | 0.055 | 0.440 | 0.220 |
| $t_{cm}$ | 0.110 | 0.055 | 0.440 | 0.165 |

Before proceeding with the selection of the design points, the size of the design domain was reduced from 9604 to 740 feasible design points by introducing the following constraints based on the expectations for the optimum design:

1) The weight was required to be between 3.0 and 4.3 lb/ft$^2$.

2) The skin near the ends of the panel was required to be thicker than the skin in the interior of the panel ($t_{sb} \geq t_{sm}$).

3) The crown of the hat stiffener in the interior of the panel was required to be thicker than the crown in the end sections of the panel ($t_{cm} \geq t_{cb}$).

### Buckling Response Surface

The STAGS model used in the analysis of the hat-stiffened panel had approximately 70,000 degrees of freedom. The panel skin and all of the elements of the stiffeners were modeled as branched shells. One linear stress and linear bifurcation buckling analysis using this model required approximately 6500 CPU s on a DEC ALPHA 200 4/166 workstation.

Because of the time required to perform each of the STAGS structural analyses, a simple linear polynomial response surface for the buckling load factor was initially constructed using 11 design points (design points 1–11 in Table 7 of Ref. 8). When the $D$-optimality criterion was used, 10 of the design points (design points 2–11) were selected. Design point 1, the nominal design given in Table 5, was selected by engineering judgement. The linear fit, constructed using these 11 points spanning through the entire design domain, for predicting the buckling load factor was very poor, with an estimate of the root mean square error (RMSE) equal to 0.61 and $Ra^2 = 0.046$. Because the buckling load factor is approximately equal to 1.0, this RMSE is very large. The parameter $Ra^2$ indicates the quality of a fit. A perfect fit is indicated by $Ra^2 = 1.0$, and $Ra^2 = 0.0$ represents a very poor fit.[6]

In an attempt to improve the accuracy of the linear response surface, a new design domain was defined around the nominal design. The thickness variables were permitted to change by $\pm 0.055$ in. from the nominal design, and the length of the end section, $d$, was permitted to change by $\pm 12$ in. Thus, each variable could have three possible values and a total of 243 design points was generated (81 of the generated points violated the $t_{sm}$ thickness constraint because the nominal design was at the lower bound for this design variable). There were 12 design points selected out of these 243 points using the $D$-optimality criterion (points 12–23 in Table 7 of Ref. 8).

The linear response surface for the buckling load factor obtained using the 12 new points had an RMSE $= 0.54$ and $Ra^2 = 0.56$, indicating that the fit was still unsatisfactory. Moreover, the $t$ statistics of the coefficients were very small. The $t$ statistic[6] is a parameter that indicates the confidence in the values of the coefficients obtained, and it is defined as the ratio between the value of a coefficient and its variance. A higher confidence level is indicated by a higher value of the $t$ statistic, which means that the value of the coefficient is much larger than its variance. Because the linear response surface models were not satisfactory, 10 design points were added to the 23 design points that were used in constructing the two linear response surface models described earlier. With these 33 design points (Table 7, Ref. 8), a full quadratic polynomial was fitted over the entire design domain. A full quadratic polynomial in five design variables has 21 coefficients. Terms in the polynomial with a low $t$ statistic were discarded as long as $Ra^2$ kept increasing. The quadratic polynomial retained 10 coefficients and is given by

$$\lambda = -4.199 + 0.1708d + 34.14t_{sm} - 0.001362d^2 - 31.98t_{sb}^2 - 0.4712dt_{sm} + 72.30t_{sm}\,t_{sb} - 95.94t_{sm}^2 - 0.759t_{cm}d + 22.43t_{cm}\,t_{sb} \quad (1)$$

For the polynomial fit in Eq. (1), RMSE $= 0.25$ and $Ra^2 = 0.82$. Furthermore, the lowest $t$ statistic was 3.17, which indicates reasonable

confidence in the coefficients. The accuracy of the response surface was also checked by constructing several response surfaces using only 32 points and then comparing the response surface predictions at the point left out with the STAGS analysis predictions at that point (a procedure known as PRESS[6]). Based on these comparisons, the quadratic response surface prediction for the buckling load factor is expected to have less than 20% error.

#### Stress Response Surface

A quadratic response surface for the midsurface compressive, spanwise stress in the skin, at the change in skin thickness between the end sections of the panel and the interior section of the panel, was also constructed. Stress values at all other locations in the panel, for all of the designs analyzed, did not exceed the maximum stress allowable. The response surface obtained with units of kilopounds per square inch is given by

$$\sigma = 1.087 - 2.011d - 95.15t_{sb} - 481.5t_{sm} + 0.01503d^2$$
$$-1.141dt_{sb} + 2.816t_{sm}d + 323.4t_{sm}t_{sb} + 813.6t_{sm}^2 \qquad (2)$$

with $Ra^2 = 0.96$ and RMSE $= 1924$ psi. The $t$ statistic for all of the coefficients was higher than 3.33. The accuracy of the response surface was also checked by the PRESS procedure, which indicated that a maximum error of 20% is expected when the stress response surface is used to estimate the spanwise midsurface compressive stresses in the skin near the thickness discontinuity.

#### Optimization Using the Response Surfaces

As indicated, the response surface for the buckling load factor $\lambda$ and the stress response surface had errors of 20%. Therefore, the required buckling load factor was increased by 20% from 1.15 to 1.38, and the safety factor on the compressive stresses was increased by 20% from 1.3 to 1.56.

The optimization problem was formulated as shown in Table 6 and solved using a reduced gradient optimizer available in Microsoft EXCEL. The optimum design obtained, subject to the constraints specified in Table 6, is presented in Table 7. Analysis of the design in Table 7 with STAGS gave a buckling load factor $\lambda_c = 1.379$ and a maximum spanwise stress $\sigma_x = -22{,}450$ psi in the skin at the boundary between the end section and the interior section of the panel. The variable cross-sectional design for the upper cover panel, obtained using the response surface approach, has a weight of 3.53 lb/ft$^2$ (Table 7) compared to a weight of 4.86 lb/ft$^2$ (Table 3) for the uniform cross-sectional design.

**Table 6 Initial optimization problem using response surfaces**

| Objective function | Min{weight} |
|---|---|
| Design variables | $d$, $t_{sb}$, $t_{sm}$, $t_{cm}$, $t_{cb}$ |
| Constraints | $\lambda > 1.38$ |
| | $\sigma < 32{,}051$, psi |
| | $t_{sb} - t_{sm} > 0$ |
| | $t_{cm} - t_{cb} > 0$ |
| | $24 < d < 48$, in. |
| | $0.110 < t_{sb} < 0.220$, in. |
| | $0.110 < t_{sm} < 0.165$, in. |
| | $0.165 < t_{cm} < 0.275$, in. |
| | $0.110 < t_{cb} < 0.220$, in. |

**Table 7 Initial optimum design obtained using response surface**

| Parameter | Optimum |
|---|---|
| $d$, in. | 30 |
| $t_{sb}$, in. | 0.165 |
| $t_{sm}$, in. | 0.110 |
| $t_{cm}$, in. | 0.165 |
| $t_{cb}$, in. | 0.110 |
| Weight, lb/ft$^2$ | 3.533 |
| $\lambda$ STAGS | 1.379 |
| $\sigma$, psi, STAGS | 22,450 |
| $\lambda$ response surface | 1.416 |
| $\sigma$, psi, response surface | 23,845 |

## Design for Updated Load Conditions

After the optimization described was completed, the design loads were updated as the overall airplane design changed. A new load case of internal pressure only, $p = 18.56$ psi, was added, and in the combined load case, the pressure loading was changed from 14.84 to 15.59 psi and the in-plane, spanwise load was changed from 4319 to 2879 lb/in. In addition, the buckling and stress safety factors were reduced to 1.0. The reduction in the buckling safety factor reflected a change in design philosophy, allowing local buckling of the skin between the design limit load and the design ultimate load.

PANDA2 was used to optimize the hat-stiffened panel with uniform cross section for the updated combined load case, and a panel weight of 4.30 lb/ft$^2$ was obtained, indicating that the updated loading condition was less severe than the initial loading condition. Moreover, Bushnell, the developer of PANDA2,[3] obtained an optimal two cross-sectional hat-stiffened panel design using PANDA2 and the design variables in Table 2. The two cross-sectional designs obtained by PANDA2 for a panel with a change in cross section specified at 24.0 in. from the ends of the panel weighed 3.71 lb/ft$^2$.

To obtain a more efficient variable cross-sectional design, STAGS was again employed. The STAGS finite element model of the hat-stiffened panel was simplified to include only one panel module, 13.83 in. wide, with symmetry conditions imposed along the sides parallel to the $x$ axis. Also, the weight calculations were refined to remove duplications in the earlier calculations due to intersecting finite elements.

The design for the updated load conditions was initiated using the optimum design obtained in the design cycle for the initial load condition as a starting point. In the optimization for the initial load condition, the thickness of the skin in the interior section of the panel, $t_{sm}$, remained at its lower limit throughout the optimization process and was not an active variable in the design. In addition, for the optimum design presented in Table 7, the webs account for approximately 40% of the total panel weight. Based on these observations, the design variable list was modified by including the web thickness $t_w$ as a design variable and by removing the thickness of the skin in the interior section of the panel, $t_{sm}$, from the design variable list.

A design domain for the updated optimization was generated around the optimum design point obtained in the preceding optimization. The design domain was limited to 162 new design points by introducing the following restrictions. The thickness of the skin in the end sections of the panel and the thickness of the stiffener crown in the interior section of the panel were permitted to change by $\pm 0.055$ in. from the earlier optimum design (Table 7). The thickness of the crown in the end sections of the panel was allowed to be twice as thick as it was for the initial combined load case to handle the new load case of internal pressure only that induces high tensile stresses in the crown near the panel ends. The stiffener web was constrained to have a thickness equal to 0.165 or 0.220 in. A thinner web would violate the buckling constraint, and a thicker web would result in unacceptably heavy designs. The distance from the panel ends to the thickness discontinuity $d$ was permitted to change by $\pm 6$ in. from the earlier optimum design value. The thickness of the skin in the interior section of the panel, $t_{sm}$, was equal to 0.110 in., and $t_{sm}$ was held constant during the optimization process. The change thickness, which was equal to 0.110 in., was also held constant during the optimization process.

The JMP program was employed to select a $D$-optimal set of 26 new design points from the 162 candidate design points. STAGS was used to conduct linear analyses of each of these 26 designs for the internal-pressure-only load case and for the combined load case. Table 8 shows the 26 designs and the results obtained from the STAGS analyses for the buckling load factors $\lambda_p$ and $\lambda_c$, for the internal-pressure-only load case and for the combined load case, respectively. The buckling load factors were obtained from a linear

**Table 8 Structural designs near initial optimum design (point 1) that were used for updated response surface optimization**

| Point no. | $d$, in. | $t_{sb}$, in. | $t_{cm}$, in. | $t_{cb}$, in. | $t_w$, in. | Weight, lb/ft$^2$ | $\lambda_p$ | $\lambda_c$ | $(\sigma_x)_{max}$, psi |
|---|---|---|---|---|---|---|---|---|---|
| 1 | 30 | 0.220 | 0.110 | 0.110 | 0.220 | 3.505 | 0.848 | 0.805 | 56,858 |
| 2 | 30 | 0.165 | 0.165 | 0.165 | 0.220 | 3.410 | 1.680 | 1.496 | 46,161 |
| 3 | 30 | 0.110 | 0.110 | 0.110 | 0.165 | 2.755 | 0.661 | 0.620 | —— |
| 4 | 36 | 0.220 | 0.220 | 0.165 | 0.165 | 3.366 | 2.565 | 1.756 | —— |
| 5 | 36 | 0.220 | 0.110 | 0.165 | 0.165 | 3.321 | 0.800 | 0.695 | —— |
| 6 | 36 | 0.110 | 0.220 | 0.165 | 0.220 | 3.341 | 1.000 | 0.893 | —— |
| 7 | 36 | 0.110 | 0.220 | 0.165 | 0.165 | 2.943 | 0.895 | 0.779 | —— |
| 8 | 36 | 0.110 | 0.110 | 0.165 | 0.220 | 3.186 | 0.865 | 0.797 | —— |
| 9 | 36 | 0.110 | 0.110 | 0.165 | 0.165 | 2.786 | 0.761 | 0.652 | —— |
| 10 | 24 | 0.220 | 0.220 | 0.165 | 0.220 | 3.602 | 2.736 | 1.206 | —— |
| 11 | 24 | 0.220 | 0.220 | 0.165 | 0.165 | 3.207 | 2.516 | 1.003 | —— |
| 12 | 24 | 0.220 | 0.110 | 0.165 | 0.220 | 3.399 | 0.870 | 0.803 | —— |
| 13 | 24 | 0.220 | 0.110 | 0.165 | 0.165 | 3.002 | 0.716 | 0.657 | —— |
| 14 | 24 | 0.110 | 0.220 | 0.165 | 0.220 | 3.322 | 1.005 | 0.906 | —— |
| 15 | 24 | 0.110 | 0.110 | 0.165 | 0.220 | 3.120 | 0.832 | 0.764 | —— |
| 16 | 36 | 0.220 | 0.165 | 0.110 | 0.165 | 3.290 | 1.452 | 1.238 | 64,761 |
| 17 | 36 | 0.220 | 0.110 | 0.110 | 0.165 | 3.212 | 0.694 | 0.664 | 66,607 |
| 18 | 36 | 0.165 | 0.220 | 0.110 | 0.220 | 3.553 | 1.698 | 1.508 | 55,149 |
| 19 | 36 | 0.110 | 0.110 | 0.110 | 0.220 | 3.189 | 0.814 | 0.769 | 58,858 |
| 20 | 30 | 0.165 | 0.165 | 0.110 | 0.220 | 3.420 | 1.661 | 1.484 | 57,009 |
| 21 | 30 | 0.110 | 0.220 | 0.110 | 0.165 | 3.334 | 0.892 | 0.890 | 63,389 |
| 22 | 30 | 0.220 | 0.220 | 0.110 | 0.220 | 4.000 | 2.705 | 1.260 | 54,627 |
| 23 | 24 | 0.165 | 0.110 | 0.110 | 0.165 | 3.262 | 0.665 | 0.623 | 66,618 |
| 24 | 24 | 0.110 | 0.220 | 0.110 | 0.165 | 3.324 | 0.893 | 0.785 | 61,609 |
| 25 | 24 | 0.110 | 0.220 | 0.110 | 0.165 | 2.926 | 0.971 | 0.874 | 56,235 |
| 26 | 24 | 0.110 | 0.110 | 0.110 | 0.165 | 2.722 | 0.650 | 0.607 | 67,113 |

bifurcation buckling analysis from a linear prestress state. For the combined load case, the internal pressure load and the spanwise compressive load were included in one load set, and the buckling load factor was applied to the combined load. The pressure-only load generated high tensile stresses in the crown of the hat stiffener due to bending. The tensile midsurface spanwise stresses in the crown calculated at 3.5 in. from the panel end for the internal-pressure-only load case are also provided in Table 8. The dashes in Table 8 indicate designs for which stress calculations were not performed.

The stress calculations performed with STAGS indicated that the stress allowable was not exceeded anywhere in the panel for the combined load case and was exceeded in the crown of the hat stiffener for the internal-pressure-only load case. For this load case, several designs failed due to large, spanwise, tensile stresses in the crown of the hat stiffener, near the ends of the panel. Furthermore, the STAGS analyses showed that for the two load cases considered in the present analysis, a simple beam analysis provides a good approximation of the stress distribution along the panel length. Because the stress calculations performed using the beam approximation are inexpensive, the approximate beam analysis was used to calculate the stresses in the crown of the hat stiffener at 3.5 in. from the panel ends for all of the 162 structures. The stress results from the approximate beam analysis were compared with the STAGS analysis stress results for 13 structures (points 1–2 and points 16–26 in Table 8). The difference between the simple beam predictions and the STAGS analysis predictions ranged from 0.1 to 6.5%.

### Approximate Buckling Analysis

The STAGS analyses for the 26 hat-stiffened cover panel designs provided in Table 8 showed that for buckling load factors less than 1.0 or close to 1.0, buckling was generally local and confined to a single element of the hat-stiffened panel, that is, only the cap of the hat stiffener or the panel skin had any appreciable deformation. This observation is demonstrated in Fig. 7, where buckling mode shapes are shown for four design points. The first buckling mode shape for the configuration defined by design point 3 and subjected to combined internal pressure and spanwise compression loading is shown in Fig. 7a. The buckling is mostly confined to the crown of the hat stiffener in the interior section of the panel. The first buckling mode for the configuration defined by design point 5, and subjected to internal pressure only is shown in Fig. 7b. For this design and load case, buckling is confined mostly to the skin near the panel ends. Figure 7c presents an example of skin buckling in the thin section of the skin near the skin thickness discontinuity. Interactive buckling modes were also predicted, but the buckling load factors for these modes were substantially greater than 1.0. An example of an interactive buckling mode shape is shown in Fig. 7d, where both the crown and the webs of the hat stiffener buckle simultaneously.

Based on the individual components of the hat-stiffened panel buckling independently for buckling load factors close to 1.0, an approximate buckling analysis was developed by representing a subregion of each component of the hat-stiffened panel as a simply supported plate. These subregions were assumed to have width $w$ equal to the width of the component of the stiffener they were representing (e.g., the width $w = 4.3$ in. was used for the crown of the hat stiffener) and length equal to the length of a half-wave of the bucking mode that corresponds to the lowest critical load value of a plate of width $w$ that is simply supported on all edges. The component with the lowest buckling load determined the buckling load for the hat-stiffened panel.

The spanwise stresses in the panel induced by the internal pressure load vary quadratically along the length of the panel. However, the stress is approximately constant over a single buckling half-wave because the length of a single buckling half-wave is much smaller than the length of the panel (see Fig. 7). Therefore, the buckling stress for a single component of the hat-stiffened panel was approximated from the buckling solution for a simply supported plate under constant load and is given by

$$\sigma_{buck} = \left(\pi^2 / tm^2 b_b^2 R^2\right)\left[m^4 D_{11} + 2(D_{12} + 2D_{66})(mnR)^2 + D_{22}(nR)^4\right] \tag{3}$$

where $b_b$ and $t$ are the width and the thickness, respectively, of the component of the hat-stiffened panel under consideration; $R = a_b/b_b$ is the ratio between the length and the width of the panel component; and $m$ and $n$ are, respectively, the number of half-waves in the direction parallel and perpendicular to the loading $N_x$. The Appendix shows that the minimum buckling stress for a simply

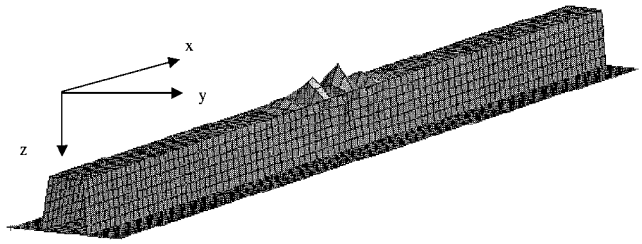


**a) Design point 3, combined internal pressure and in-plane compression load case**

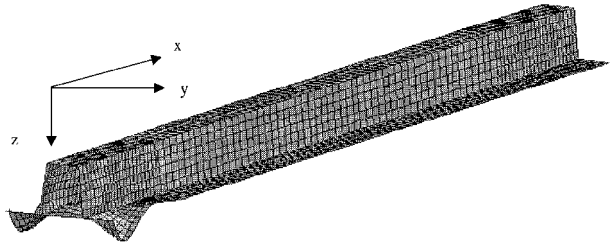


**b) Design point 5, internal pressure load case**

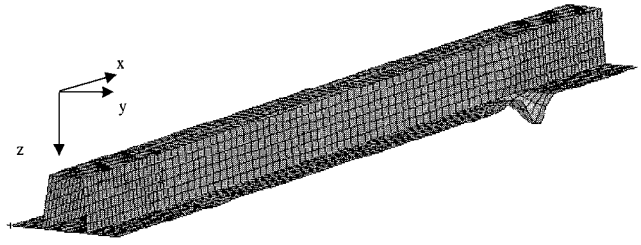


**c) Design point 11, combined internal pressure and in-plane compression load case**

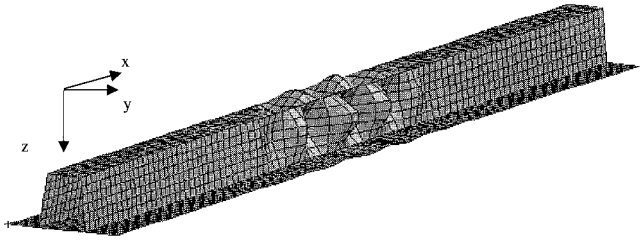


**d) Design point 2, combined load case**

**Fig. 7 Examples of buckling modes predicted by STAGS analyses; design point numbers refer to Table 8.**

supported plate with fixed width $b_b$ and thickness $t$ is achieved for a length

$$a_b = (D_{11}/D_{22})^{\frac{1}{4}} b_b \tag{4}$$

Substituting Eq. (4) and the material properties given in Table 1 into Eq. (3) gives the approximate buckling stress for an individual component of the hat-stiffened panel:

$$\sigma_{\text{buck}} = 2.25 \times 10^8 (t/b_b)^2 \tag{5}$$

An approximation for the buckling load factor was obtained by dividing the approximate buckling stress given by Eq. (5) by the approximate applied stress, determined from the simple beam analysis discussed before. The approximate buckling load factor is defined as $\lambda = \sigma_{\text{buckling}}/\sigma_{\text{applied}}$. A value of $b_b$ of 8.0 in. was used in the calculations of $\sigma_{\text{buck}}$ for the skin near the ends of the panel and for the thin skin section at the thickness discontinuity ($b - w_2$ in Fig. 5). To evaluate the buckling stress in the crown of the hat stiffener, the value of $b_b$ was set equal to 4.3 in. ($w$ in Figs. 5 and 6).

Comparison of the buckling load factor obtained using the approximate analysis with the buckling load factor predicted by STAGS for the 26 designs provided in Table 8 indicated that the approximate buckling load factor underestimated the panel buckling resistance. This result was expected because the neighboring plate elements provide more boundary restraint than is provided by a simple support boundary condition. Also, the stresses are not constant over the length of a component subregion, and the buckling load factor was calculated in the approximate analysis on the basis of the maximum stress over the length $a_b$. The buckling load factors predicted by the approximate analysis were up to 75% smaller than the buckling load factors predicted by STAGS. To improve the buckling load factor predictions obtained using the approximate beam-plate analysis, the STAGS results were used to fit a scale factor (as a single-term response surface) to the buckling load factor in each critical region of the panel. The computed scale factors are provided in Table 9. The combined load condition was critical for buckling for all of the designs considered, and so the response surface was generated for this load case only. The buckling load factors predicted by the approximate analysis combined with the scale factors provided in Table 9 had a maximum error of 10% for panels whose buckling deformations were primarily localized to one element of the hat-stiffened panel. The approximate analysis generally overestimated the buckling load factor for panels that activate an interactive buckling response. For these structures, the buckling load factors predicted by the approximate analysis and by the STAGS analysis were well above 1.0.

**Table 9 Scale factors for combined load case buckling load factor, $\lambda_c$**

| Buckling location | Scale factor |
|---|---|
| Cap in the interior section | 1.804 |
| Skin the interior section | 3.943 |
| Skin at the end section | 1.313 |

**Table 10 Minimum weight structure design**

| Design variable | Value |
|---|---|
| $d$, in. | 24.0 |
| $t_{\text{sb}}$, in. | 0.165 |
| $t_{\text{cm}}$, in. | 0.165 |
| $t_{\text{cb}}$, in. | 0.220 |
| $t_w$, in. | 0.165 |
| Weight, lb/ft$^2$ | 2.755 |

### Minimum Weight Structure

The four three-level design variables $d$, $t_{\text{sb}}$, $t_{\text{cb}}$, and $t_{\text{cm}}$ and the two-level design variable $t_w$ generate a design domain of 162 points. All 162 designs were analyzed using beam theory to determine the stresses and the scaled plate-beam approximation to determine the buckling load factor. The most promising design was identified and then checked by a STAGS analysis. The optimum design, found by inspection of the approximate analysis predictions, is given in Table 10. The structure shown in Table 10 weighs 2.75 lb/ft$^2$. The maximum spanwise stress predicted by the approximate analysis was a tensile stress of 44,101 psi, in the crown of the hat stiffener, for the pressure-only load condition. The minimum buckling load factor obtained from the approximate buckling analysis was for the combined load condition and had a value $\lambda_c = 0.97$. This buckling load factor corresponds to skin buckling in the interior region of the panel.

The design provided in Table 10 was further checked for adequacy using a STAGS linear bifurcation buckling analysis from both a linear prestress state and a nonlinear prestress state. Both analyses were conducted for the combined load case, with both the internal pressure load and the in-plane compression load applied on one load set. The buckling load factor obtained from the analysis is, therefore, applied to both loads. The STAGS linear bifurcation buckling analysis from a linear prestress state predicted a buckling load factor of $\lambda_c = 0.93$. The buckling mode was predominantly buckling of the thin skin section at the axial location where the cross section changes and is consistent with the buckling mode predicted by the approximate analysis. The predicted maximum tensile stress in the crown of the hat stiffener near the ends of the panel was 45,097 psi.

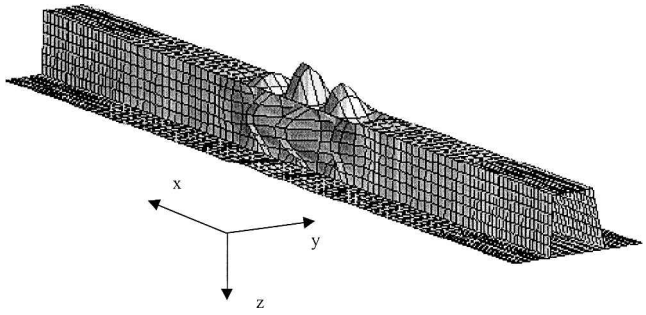


**Fig. 8 Linear bifurcation buckling mode from nonlinear prestress state of optimal design for combined loading condition.**

A linear bifurcation analysis executed from a nonlinear prestress state, and with both loads applied on one load set, predicted a buckling load factor $\lambda_c = 1.11$. The corresponding buckling mode shape is shown in Fig. 8. The buckling mode is interactive, and the crown and the web of the hat stiffener buckle simultaneously. The interactive buckling mode predicted by the bifurcation analysis conducted from a nonlinear prestress state corresponds to the ninth buckling mode found by the bifurcation analysis conducted from a linear prestress state. The buckling load factor predicted by the bifurcation analysis from a nonlinear prestress state is 14% higher then the buckling load factor predicted from a bifurcation buckling analysis executed from a linear prestress state.

## Concluding Remarks

A design study for structural optimization of a hat-stiffened laminated composite panel concept for the upper cover panel of a typical passenger bay of a BWB transport airplane is presented. The hat-stiffened panel was subjected to internal pressure load and to combined internal pressure and in-plane loads. The structural optimization problem was formulated using weight as the objective function with stress and buckling constraints. The initial optimization was conducted for a design having uniform properties in the spanwise direction using the PANDA2 program. The design was then refined to allow for variable cross section using a more flexible design procedure that combined the STAGS finite element analysis program with response surface approximations for the stresses and for the buckling loads.

The design loads and safety factors were changed during the design process, but the knowledge of the design space gained from the first load case allowed an easy update to the optimum design. Furthermore, in the small region in the design space that was used for updating the design, simple beam and plate approximations were used with simple correction factors obtained from STAGS to generate response surface approximations for the stresses and for the buckling loads.

The design study demonstrated the use of three levels of analysis models and the use of response-surface approximations for integrating the analysis models into the design process. This process resulted in a reduction in the weight of the hat-stiffened laminated composite panel concept from 4.30 to 2.75 lb/ft$^2$. The hat-stiffened panel concept proved to be a valid alternative to the thick sandwich concept because it achieved a weight of less than 3.0 lb/ft$^2$.

## Appendix: Buckling Stress of an Orthotropic Simply Supported Plate

The buckling stress of an orthotropic simply supported plate, under a constant compressive stress $\sigma_x$ as in Fig. A1, is given by

$$\sigma_{\text{buck}} = \left(\pi^2 / tm^2 b_b^2 R^2\right)\left[m^4 D_{11} + 2(D_{12} + 2D_{66}) \times (mnR)^2 + D_{22}(nR)^4\right] \quad \text{(A1)}$$

where $t$ is the thickness of the plate; $R = a_b/b_b$ is the ratio between the length $a_b$ and the width $b_b$ of the plate; $D_{11}$, $D_{22}$, $D_{12}$, and $D_{22}$ are the bending stiffness material properties of the orthotropic plate; and $n$ and $m$ are the number of half-waves, respectively, in the direction perpendicular to the loading and in the direction parallel to the loading.

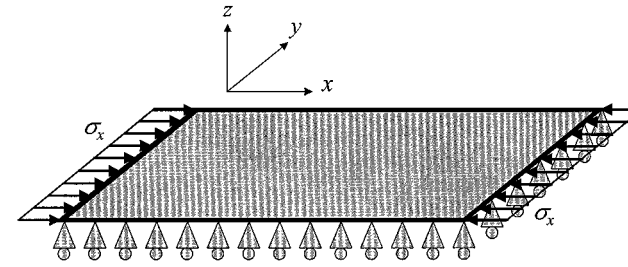


**Fig. A1 Simply supported plate under constant compressive stress $\sigma_x$.**

From Eq. (A1) it is possible to find the length $a_b$ of an orthotropic plate that minimizes $\sigma_{\text{buck}}$ for a given width $b_b$ by performing

$$\frac{\partial \sigma_{\text{buck}}}{\partial a_b} = 0 \quad \text{(A2)}$$

which gives

$$a_b = (D_{11}/D_{22})^{\frac{1}{4}}(m/n)b_b \quad \text{(A3)}$$

When Eq. (A3) is substituted into Eq. (A1), the minimum buckling load $\sigma_{\text{buck}}$ is

$$\sigma_{\text{buck}} = \pi^2 n^2\left[2\sqrt{D_{11}D_{22}} + 2(D_{12} + 2D_{66})\right]/tb_b^2 \quad \text{(A4)}$$

The minimum $\sigma_{\text{buck}}$ is then obtained for $n = 1$. The fact that $\sigma_{\text{buck}}$ in Eq. (A4) does not depend on $m$ suggests that there is an infinite number of plate lengths $a_b$, one for each value of $m$ in Eq. (A3), for which an orthotropic plate of width $b_b$ achieves its minimum possible buckling load given in Eq. (A4) for $n = 1$. Without loss of generality the value for $m$ is chosen as $m = 1$ so that the minimum buckling load $\sigma_{\text{buck}}$ for an orthotropic plate of width $b_b$ is

$$\sigma_{\text{buck}} = \pi^2\left[2\sqrt{D_{11}D_{22}} + 2(D_{12} + 2D_{66})\right]/tb_b^2 \quad \text{(A5)}$$

The corresponding length value is

$$a_b = (D_{11}/D_{22})^{\frac{1}{4}}b_b \quad \text{(A6)}$$

## Acknowledgment

This work was supported in part by NASA Grants NAG1-1669 and NAG1-2000. Helpful discussions with members of the blended wing–body team, George Rowland and Art Hawley of The Boeing Company, Long Beach, and Peter Lissaman of the California Institute of Technology are gratefully acknowledged. The authors also appreciate the useful suggestions and guidance from David Bushnell of Lockheed Martin Corporation.

## References

[1] Mason, B. H., Haftka, R. T., Johnson, E. R., and Farley, G. L., "Variable Complexity Design of Composite Fuselage Frames by Response Surfaces Techniques," *Thin Wall Structures*, Vol. 32, No. 4, 1998, pp. 235–261.

[2] NASA Contracts NAS1-18862, NAS1-20014, and NAS1-20546.

[3] Bushnell, D., "PANDA2—Program for Minimum Weight Design of Stiffened, Composite, Locally Buckled Panels," *Computers and Structures*, Vol. 25, No. 4, 1987, pp. 469–605.

[4] Rankin, C. C., Brogan, F. A., Loden, W. A., and Cabiness, H. D., "STAGS User Manual, Version 3.0," Rept. LMSC P032594, Lockheed Martin Missiles and Space Co., Inc., Advanced Technology Center, Palo Alto, CA, June 1998.

[5] EXCEL 5.0, Microsoft Corp., 1997.

[6] Myers, R. H., and Montgomery, D. C., *Response Surface Methodology*, Wiley, New York, 1995, pp. 29–31.

[7] JMP, Ver. 3.1, SAS Inst., Cary, NC, 1995.

[8] Vitali, R., Park, O., Haftka, R. T., and Sankar, B. V., "Structural Optimization of a Hat-Stiffened Panel by Response Surface Techniques," *Proceedings of the 39th AIAA/ASME/ASCE/AHS/ASC Structures, Structural Dynamics and Materials Conference*, Vol. 4, AIAA, Reston, VA, 1997, pp. 2983–2993.